AUTOMATIC POSE ESTIMATION OF IMAGERY USING FREE-FORM CONTROL LINEAR FEATURES

A. F. Habib[a], S. W. Shin[a], M. F. Morgan[a]

[a] Department of Civil and Environmental Engineering and Geodetic Science, The Ohio State University,
470 Hitchcock Hall, 2070 Neil Avenue, Columbus, OH 43210, USA - (habib.1, shin.111, morgan.465)@osu.edu

Commission III, WG III/1

ABSTRACT:

Automatic Single Photo Resection (SPR) remains to be one of the challenging problems in digital photogrammetry. Visibility and uniqueness of distinct control points in the input imagery limit robust automation of the pose estimation procedure. Recent advances in digital photogrammetry mandate adopting higher-level primitives such as free-form control linear features for replacing traditional control points. Linear features can be automatically extracted from the image space. On the other hand, object space control linear features can be obtained from an existing GIS layer containing 3-D vector data such as road network, or from terrestrial Mobile Mapping Systems (MMS). In this paper, we present a new approach for simultaneously determining the position and attitude of the involved imagery as well as the correspondence between image and object space features. This approach does not necessitate having one to one correspondences between image and object space primitives, which makes it robust against changes and/or discrepancies between them. This characteristic will be helpful in detecting changes between object and image space linear features (e.g. due to temporal effects). The parameter estimation and matching follow an optimal sequential procedure that depends on the magnitude and direction of image space displacements resulting from incremental changes to the Exterior Orientation Parameters (EOP). Experimental results using real data proved the feasibility and robustness of our approach, especially when compared to those obtained through traditional manual procedures. Changes and/or discrepancies between the data sets are detected and highlighted through consistency analysis of the resulting correspondences.

1. INTRODUCTION

The majority of traditional computational procedures in photogrammetry rely on the correspondence between point primitives. With the recent advances in digital photogrammetry, more emphasis should be oriented towards using higher-level primitives in photogrammetric orientation procedures. There has been a substantial body of work dealing with the use of analytical linear features (e.g. straight lines and conic curves) in photogrammetric orientation (Habib et al, 2000b), (Habib, 1999), (Mikhail, 1993), (Mulawa and Mikhail, 1988). On the other hand, very few papers addressed the use of free-form linear features (Zalmanson, 2000), (Habib and Novak, 1994). However, the suggested approaches by these authors assume the knowledge of the correspondence between the object and image space features.

SPR is a photogrammetric procedure to determine the EOP of aerial images, which is a prerequisite task for variety of applications such as surface reconstruction, ortho-photo generation and object recognition. Traditionally, SPR is performed using signalised control points, which have to be established prior to the flight mission. Radiometric problems and small signal size in terms of number of pixels limit the robustness of the automation process (Gülch, 1994). Mikhail et al (1994) used radiometric models of the object space control points and tried to determine their instances in the image. Very good approximations of EOP are required in this approach to ensure small "pull-in" range. Other approaches (Haala and Vosselman, 1992; Drewniok and Rohr, 1997) employed relational matching of points. Relations between points are not

as well-defined as those between linear or higher-level features. In this research, the SPR problem is solved using free-form linear features in the image and object space without knowing the correspondence between these entities.

Presently, there is a great motivation for exploiting and integrating various types of spatial data. This motivation is fuelled by the availability of new acquisition systems such as aerial and terrestrial mobile mapping systems and airborne laser scanners. The suggested approach in this research, for automatic SPR, has the potential of incorporating object space information acquired from a terrestrial mobile mapping system, line maps, or a GIS database with aerial imagery. The fusion of these data will enable point-to-point correspondence between image and object space linear features. This type of correspondence facilitates change detection applications that are well suited for automation. The Modified Iterated Hough Transform (MIHT) for robust parameter estimation (Habib et al, 2000a) is used to estimate the EOP as well as matching image and object space points along the involved linear features.

In the following section, a brief review of the traditional Hough transform, the newly developed MIHT for robust parameter estimation technique and its application in SPR are presented. In Section 3, the methodology of the suggested approach is outlined, including the optimum sequence for parameter estimation and change detection, followed by experimental results using real data. Finally, conclusions and recommendations for future research are presented.

2. BACKGROUND

2.1 The Hough Transform

Hough (1962) introduced a method for parameters estimation by way of a voting scheme. The basic principle behind this approach was to switch the roles of parameters and spatial variables. Hough transform is usually implemented through an accumulator array, which is an n-dimensional, discrete space, where n is the number of parameters under consideration. In this array, the cell with the maximum number of hits yields the parameters we are looking for. The variables contributing to the peak in the accumulator array can be tracked and identified. For more details, the reader can refer to (Leavers, 1993).

2.2 The Modified Iterated Hough Transform (MIHT) for Robust Parameter Estimation

Hough transform can be modified and used to estimate the parameters of a mathematical model relating entities of two data sets. In this approach, we assume no knowledge of correspondence and do not require complete matching between entities. As a result of the parameter estimation, the correspondence is implicitly determined. The method is outlined as follows.

First, a hypothesis is generated that an entity in the first data set corresponds to an entity in the second one. The correspondence between conjugate entities of the data sets is expressed by a mathematical function. Using the hypothesized match, this mathematical function yields an observation equation(s). The parameters of the mathematical relation can be estimated simultaneously or sequentially, depending on the number of hypothesized matches simultaneously considered. All possible entity matches are evaluated, and the results (parameter estimations) are represented in an accumulator array. The accumulator array will exhibit a peak at the location of the correct parameter solution. By tracking the matched entities that contributed to the peak, the correspondence is determined.

The number of parameters being simultaneously solved for determines the dimension of the accumulator array. In order to solve n parameters simultaneously, one must utilize the number of hypothesized entity matches needed to generate the required n equations. However, this approach is not practical. Simultaneous evaluation of all permutations of entities leads to combinatorial explosion. For example, if there are x entities in data set one and y entities in data set two, solving n parameters simultaneously would lead to $\dfrac{xy!}{(xy-n)!\ n!}$ combinations (assuming that each matching hypothesis yields one equation). In addition, the memory requirements of an n dimensional accumulator array create another problem.

Random Sample Consensus (RANSAC) is another alternative for fitting a model to experimental data (Fischler and Bolles, 1981). Rather than using large data set with high percentage of blunders and trying to eliminate invalid matched, RANSAC starts by a and consistent data set whenever possible. This method is quite similar to using the modified Hough transform discussed in the previous paragraph, to simultaneously solve for all the involved parameters.

An alternative approach is to solve for the parameters sequentially in an iterative manner (starting from some initial/approximate values), updating the approximations at each step. Consequentially, the accumulator array becomes one-dimensional and the memory problem disappears. Also, if there are x elements in data set one and y elements in data set two, the total number of evaluated entity matches becomes xy, reducing the computational complexity of the problem. After each iteration, the approximations are updated and the cell size of the accumulator array can be reduced to reflect the improvement in the quality of the approximate values of the unknown parameters. In this manner, the parameters can be estimated with high accuracy. The convergence of this approach depends on the correlation among the parameters and the non-linearity of the transformation function. Highly non-linear transformations have a slower convergence rate and would require more iterations.

The basic steps for implementing the MIHT for parameter estimation are as follows: 1) A mathematical model is established that relates corresponding entities of two data sets. The relation between the data sets can be described as a function of its parameters: $f(p_1,\ p_2,...p_n)$. 2) An accumulator array is formed for the parameters. The accumulator array is a discrete tessellation of the range of expected parameter solutions. The dimension of the accumulator array depends on the number of parameters to be simultaneously solved, which is related to the number of entity pairings simultaneously considered as well as the number of equations provided by a single matching hypothesis. 3) Approximations are made for parameters which are not yet to be determined. The cell size of the accumulator array depends on the quality of the initial approximations; poor approximations will require larger cell sizes. 4) Every possible match between individual entities of the two data sets is evaluated, incrementing the accumulator array at the location of the resulting solution. 5) After all possible matches have been considered, the maximum peak in the accumulator array will indicate the correct solution of the parameter(s). Only one peak is expected for a given accumulator array. 6) After each parameter is determined (usually in a sequential manner), the approximations are updated. For the next iteration, the accumulator array cell size is decreased, and steps 2-6 are repeated. Detailed explanation about the MIHT can be found in (Habib et al, 2000a) and (Habib et al, 2001).

2.3 Single Photo Resection (SPR)

In SPR, the collinearity model (Equation 1) is used to relate points in the image with corresponding points in the object space, and this relation is expressed as a function of the EOP. Traditionally, the parameters are estimated by way of a least squares adjustment involving measured control points in the image. At least three control points are required to estimate the six EOP. The introduction of more than three points increases the redundancy and strengthens the solution of the parameters.

$$\begin{bmatrix} x_i - x_p \\ y_i - y_p \\ -c \end{bmatrix} = \lambda\ R^T\left(\omega, \phi, \kappa\right) \begin{bmatrix} X_i - X_0 \\ Y_i - Y_0 \\ Z_i - Z_0 \end{bmatrix} \tag{1}$$

where

λ: Scale
x_i, y_i: Image coordinates of ith point
X_i, Y_i, Z_i: Object coordinates of ith point
x_p, y_p, c: The camera interior orientation parameters.
$X_0, Y_0, Z_0, \omega, \phi, \kappa$: The EOP of the camera exposure station.

3. METHODOLOGY

3.1 Optimum Sequence for Parameter Estimation and Initial Correspondence Determination

To execute the MIHT for SPR, we must first make a decision regarding the optimum sequence for parameter estimation that guarantees quick and robust convergence to the correct solution.

Various image regions are affected differently by changes in the associated EOP. Some parameters have low influence on some regions while having larger influence on others. Therefore, a certain region in the image space would be useful for estimating some parameters if they have a large influence at that region while other parameters have minor or almost no influence at the same region. Moreover, optimum sequence should not affect previously considered regions/parameters. Conceptually, optimal sequential parameter estimation should follow the same rules of empirical relative orientation on analogue plotters (Slama, 1980). The following paragraph deals with how to determine the optimum sequence for parameter estimation together with the corresponding regions for their estimation.
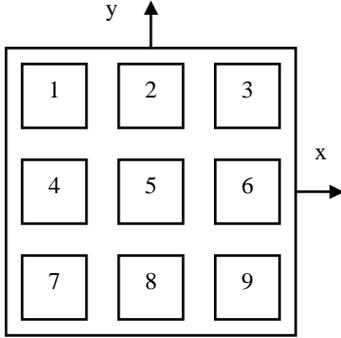

Figure 1: Image partitioning.

For such objective, we have divided the image into nine regions labelled from 1 to 9 as shown in Figure 1. Regions 2, 5 and 8 have small x coordinate values (i.e. $x_2 \approx x_5 \approx x_8 \approx 0$), while regions 4,5 and 6 have small y coordinate values (i.e. $y_4 \approx y_5 \approx y_6 \approx 0$). The collinearity equations (Equations 1) have been linearized and reduced by assuming small rotation angles, which is the case of vertical aerial photographs (Equations 2).

$$e_x \approx \frac{c}{H} dX_0 + \frac{x}{H} dZ_0 - \frac{xy}{c} d\omega + (c + \frac{x^2}{c}) d\phi + y \, d\kappa \quad (2)$$

$$e_y \approx \frac{c}{H} dY_0 + \frac{y}{H} dZ_0 - (c + \frac{y^2}{c}) d\omega + \frac{xy}{c} d\phi - x \, d\kappa$$

In Equations 2, the terms e_x and e_y represent image space displacements in the x and y directions resulting from incremental changes in the EOP (dX_0, dY_0, dZ_0, dω, dϕ, dκ). It has to be mentioned that Equations 2 are not used for the parameter estimation. Instead, we will use them to identify the influence of the EOP on various regions in the image (Figure 1). Table 1 summarises the effect of incremental changes in the EOP on the nine image regions (Figure 1).

By analysing Table 1 and following the previously mentioned rules at the beginning of this section, the optimum sequence for parameter estimation is as follows:
1. Use points in region 5, to estimate X_0 and Y_0.
2. Use x-equations of points in regions 2 and 8, and y-equations of points in regions 4 and 6, to estimate κ.
3. Use x-equations of points in regions 4 and 6, and y-equations of points in regions 2 and 8, to estimate Z_0.
4. Use points in regions 1, 3, 7 and 9 to estimate ω and ϕ.

This sequence will be repeated, after updating the initial values for the parameters with the estimated ones. The procedure can be described in the following steps.

Sweep 1:
- Establish approximations for Z_0, ω, ϕ and κ.
- Determine the range and the cell size of the accumulator array for (X_0, Y_0), depending on the quality of the approximations of the other parameters.
- Using the collinearity model, solve X_0, Y_0 for every combination of object point with one image point in region 5.
- At the location of each solution, increment the corresponding cell of the accumulator array.
- After considering all possible combinations, locate the peak or maximum cell of the accumulator array. That cell has the most likely values of X_0 and Y_0.

Sweep 2:
Repeat sweep #1 for (κ), (Z_0) and (ω, ϕ) updating the approximations of the parameters, while using the appropriate regions that was determined earlier.

Sweep 3:
Decrease the cell size of the accumulator arrays for (X_0, Y_0), (κ), (Z_0) and (ω, ϕ) to reflect the improvement in the quality of the approximate EOP. Then, repeat sweeps 1–3 until the parameters converge to the desired precision.

Table 1: The influence of different image regions on the parameters.

Region	dX_0		dY_0		dZ_0	
	x eq.	y eq.	x eq.	y eq.	x eq.	y eq.
1	c/dZ	0	0	c/dZ	$-x$/dZ	y/dZ
2	c/dZ	0	0	c/dZ	0	y/dZ
3	c/dZ	0	0	c/dZ	x/dZ	y/dZ
4	c/dZ	0	0	c/dZ	$-x$/dZ	0
5	c/dZ	0	0	c/dZ	0	0
6	c/dZ	0	0	c/dZ	x/dZ	0
7	c/dZ	0	0	c/dZ	$-x$/dZ	$-y$/dZ
8	c/dZ	0	0	c/dZ	0	$-y$/dZ
9	c/dZ	0	0	c/dZ	x/dZ	$-y$/dZ

Region	dω		dφ		dκ	
	x eq.	y eq.	x eq.	y eq.	x eq.	y eq.
1	xy/c	$-c-y^2$/c	$c+x^2$/c	$-xy$/c	y	x
2	0	$-c-y^2$/c	c	0	y	0
3	$-xy$/c	$-c-y^2$/c	$c+x^2$/c	xy/c	y	$-x$
4	0	$-c$	$c+x^2$/c	0	0	x
5	0	$-c$	c	0	0	0
6	0	$-c$	$c+x^2$/c	0	0	$-x$
7	$-xy$/c	$-c-y^2$/c	$c+x^2$/c	xy/c	$-y$	x
8	0	$-c-y^2$/c	c	0	$-y$	0
9	xy/c	$-c-y^2$/c	$c+x^2$/c	$-xy$/c	$-y$	$-x$

One has to note that the lack of features in any of the nine regions may only slow the process. The reason is that all EOP affect all regions but with different magnitudes. Only the maximum influences/contributions are represented in Table1.

By tracking the paired image and object points that have contributed to the peak in the accumulator array for the final iteration, the correspondence problem is solved. The resulting matches between the object and image space features are used in a simultaneous least-squares adjustment to solve for the EOP. It has to be mentioned that the obtained correspondences are for low-level objects (i.e. between points). The following section explains the consistency check we implemented to identify the high level correspondence (i.e. between linear features) in addition to highlighting discrepancies (changes) between object and image space features.

3.2 Feature to Feature Correspondence and Change Detection

So far, we established the following:
- EOP of the image under consideration, and
- Point-to-point correspondences between object and image space linear features.

Now, we will proceed by performing a consistency check between these features using the feature labels. The consistency check has four steps:

Step1: Feature to feature correspondence
We check the label of the features containing the matched object and image space points. Considering the frequency of the matched labels, one can establish the correspondence between the image and object space features.

Step 2: Object to image space projection of non-matched object points
Using the estimated EOP and the ground coordinates of non-matched object points, one can compute the corresponding image coordinates. The standard deviation of the computed image coordinates can be estimated using error propagation.

Step 3: Distance computation
The closest distance, as well as the associated standard deviation, between the projected image points in step 2 and the closest points along the corresponding image space features is computed. One should note that the image to object feature correspondence is already established in step 1.

Step 4: Blunder and change detection
If the distance is greater than a predefined threshold (e.g. three times the associated standard deviation), we label these points as either blunders or changes between object and image space features. Single occurrences of non-matching points are identified as blunders while successive occurrences of the non-matching points are labelled as change (discrepancies).

Figure 2 is a schematic drawing for illustrating the concept of the consistency check. In this figure, points i_1 to i_{10} are the projected data points along a linear feature from the object space into the image space, while points j_1 to j_{17} are image data points along the corresponding linear feature in the image space. Consider points i_1, i_6, i_7, i_8 and i_{10} to be correctly matched with points j_1, j_{11}, j_{13}, j_{15} and j_{17}, respectively; while points i_2, i_3, i_4, i_5 and i_9 do not have matching entities in the image space. Instead, their closest points in the second data set along the corresponding linear feature are points j_3, j_5, j_7, j_9 and j_{16}, respectively. In order to distinguish between the consistent changes and blunders, non-matching points along the linear feature are segmented and labelled. From this analysis, the pair (i_9, j_{16}) will be considered as one label and the pairs (i_2, j_3) to (i_5, j_9) will be considered as another label. The former label will

be considered as blunder because it has only one change pair, while the latter will be highlighted as a consistent change. For consistent changes, the longitudinal distance along the linear feature as well as the average lateral distance will be computed as the change attributes, Figure 2.
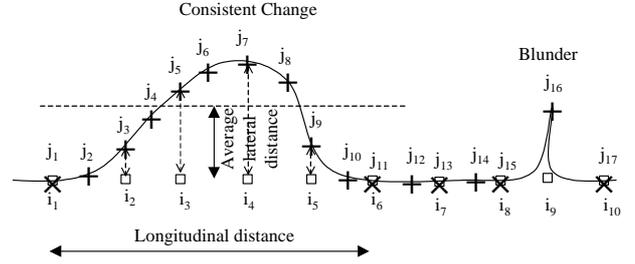

Figure 2: Consistency check between the object and image data points. The rectangular points with labels i_1 to i_{10} are the projected object space points along a linear feature into the image space, while the crosses with labels j_1 to j_{17} are the points along the corresponding linear feature in the image space.

4. EXPERIMENTS/RESULTS

Experiments have been conducted using real data. To carry out the outlined methodology in the previous section, one should have:

- A sequence of 3-D points along the ground control features.
- A sequence of 2-D points along the image features.
- The interior orientation parameters (IOP) of the camera.

Once again, the suggested algorithm does not require full correspondence between the object and image space features. The main requirement is having enough common features between the two data sets. The input data and the results are presented in the following paragraphs.

In the area covered by the aerial image, there exist a number of major and secondary roads. The object space roads, represented as a sequence of 3-D points, were extracted from a photogrammetric stereo model containing the image under consideration. Two data sets in the object space with different number of roads had been digitised. A 2-D view of the 3-D road network can be seen in Figures 4-a and 4-b. To complete the data set, a 2-D point sequence along the image road network must be extracted. In a digital environment, the extraction process can be established by applying a dedicated operator (e.g. Canny or any other operator for road network extraction). In this work however, 2-D image features have been manually digitised, Figure 3-c. Another data set in the image space had been obtained by introducing digitisation errors (Figure 3-d) to check the ability of the suggested system to detect those changes. By combining different data sets from the object and image space, we conducted four experiments, Table 2.

From Table 2, one can see that image space has much more data available than the object space. After carrying out the experiments, matched points were used to estimate the EOP in a simultaneous least-squares adjustment. The estimated EOP are listed in Table 3, together with the their initial (approximate) values. These values can be obtained from navigation data. However, very rough knowledge about the initial values of EOP

is required in this approach as listed in Table (3). Results from manual SPR are also listed in the same table. One can see that the results from the traditional manual orientation and our approach (even in Experiment 4 where fewer object space roads were used and digitisation errors were introduced in the image space features) are comparable. In addition to the estimated parameters, we had obtained the correspondences between points in image and object space.

Table 2: Experiments Summary.

			Object space data sets			
			O1 (Fig. 4-a)		O2 (Fig. 4-b)	
			15 roads	1572 points	5 roads	799 points
Image space data sets	I1 Fig. 4-c	15 roads 55178 points	Experiment 1		Experiment 2	
	I2 Fig. 4-d	15 roads 63397 points	Experiment 3		Experiment 4	

(a)   (b)
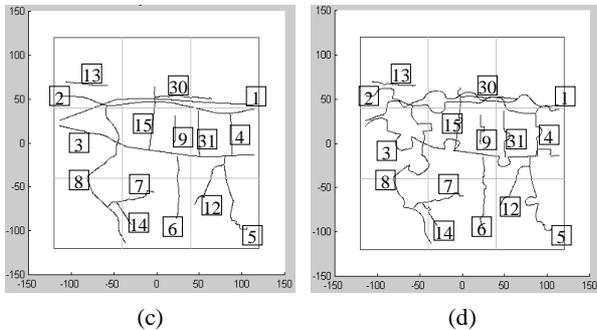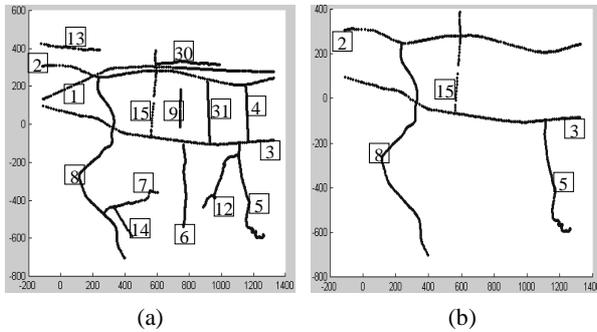

(c)   (d)

Figure 3: Object space linear features O1 (a), and O2 (b), and image space linear feature without digitisation errors I1 (c) and with digitisation errors I2 (d). Roads are labelled for further references.

The correspondence between the image and the object space linear features as well as the consistency check described in section 3.2 have been performed. All the roads were reliably matched (see Figure 3). In this figure, corresponding road segments were given the same label. One should notice that we had realised the correct correspondences between higher level entities (road segments). Even when there is no one to one correspondence between higher-level image and object space entities (as in experiment 4, where 10 out of 15 road segments in the image space are not present in the object space), correspondences are reliably obtained. Moreover, the quality of the estimated parameters did not deteriorate. The 10 roads in the

image space that had no correspondences in the object space in experiment 4 will be considered changes, as they belong to the same boundary of the object space entities that had been examined. In the next paragraph, we are examining changes that occurred locally between object and image space entities.

Table 3. Estimated EOP and their initial (approximate) values together with the results from manual SPR.

	X_0(m)	Y_0(m)	Z_0(m)
Manual	600.00	-26.781	1014.894
Appx.	450.0	100.0	900.0
Exp. 1	599.762	-26.937	1014.842
Exp. 2	599.797	-26.663	1014.699
Exp. 3	599.722	-26.974	1014.818
Exp. 4	599.245	-27.081	1014.754
	ω°	ϕ°	κ°
Manual	0.584667	-0.867300	1.191474
Appx.	9.0	-9.0	10.0
Exp. 1	0.590318	-0.872063	1.185914
Exp. 2	0.572123	-0.871997	1.182790
Exp. 3	0.589120	-0.870109	1.189792
Exp. 4	0.594399	-0.895585	1.183058

Non-matched points in the object space, after being projected into the image space, were significantly far from any of the points in the image space. Therefore all of them were considered as discrepancies. Among these non-matched points consecutive points were segmented and the longitudinal and the lateral distances from the corresponding road line were computed. Results from experiment 4 are listed in Table 4. We can see that the changes had been reliably detected.

Table 4. Changes (discrepancies) between image and object space linear features, experiment 4.

Object space Road ID	Number of points	Location			Lateral distance (m)	Longitudinal distance (m)
		X (m)	Y (m)	Z (m)		
2	3	-70.81	309.98	34.18	1.69	16.02
2	17	56.71	290.27	37.23	56.49	211.53
2	19	403.81	263.37	43.59	57.46	141.1
2	25	855.49	248	53.05	67.6	291.22
2	19	1227.19	222.05	60.53	40.61	148.97
3	13	1238.2	-91.28	67.05	44.96	114.61
3	4	910	-104.28	61.59	28.59	30.53
3	7	527.42	-64.31	55.89	30.97	72.42
3	13	199.75	32.54	47.81	41.62	81.51
3	12	-16.3	74.74	42.04	65.7	149.53
5	13	1167.07	-399.73	76.26	23.1	49.28
5	4	1169.49	-444.77	76.8	1.04	13.29
5	8	1199.87	-564.32	84.22	10.8	12.52
5	10	1259	-592.19	94.94	6.84	16.94
8	17	302.33	87.72	46.44	27.6	60.32
8	31	274.23	-141.86	51.63	56.78	105.73
8	27	240.81	-451.65	58.09	31.65	115.76
15	8	590.49	351.71	46.08	14.74	28.01

Examples of changes, which were detected, are shown in Figure 4. It has to be noted that all the changes were reliably detected and their existence does not contribute to the estimated parameters. Therefore, we realised a robust estimator for the

EOP and for obtaining the correspondence between the two data sets in addition to reliably highlighting the changes.
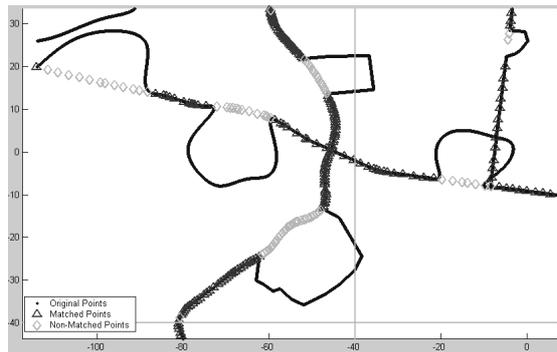

Figure 4. Example of detected changes between road segments in image and object space.

5. CONCLUSIONS AND RECOMMENDATIONS FOR FUTURE WORK

The MIHT for robust parameter estimation technique has been used to perform SPR for real data using free-form control linear features without knowing the correspondence between image and object space primitives. The proposed technique robustly estimates the parameters. In other words, the parameters are estimated using common features in both data sets (object and image space features); while non-corresponding entities are filtered out prior to the parameter estimation. An optimum sequence for parameter estimation and the associated image regions had been established and implemented. The proposed method has successfully established the feature-to-feature correspondence between the image and object space. It has also highlighted discrepancies (changes) between the object and image space road network and provided a quantitative measure indicating the amount of the change. The proposed system has the capability of integrating aerial imagery with GIS data or terrestrial mobile mapping system for decision-making purposes (e.g. re-mapping of road network). In this way, newly acquired aerial imagery can undergo SPR using available control information from a terrestrial mobile mapping system, previous imagery, GIS database or line maps. Currently, we are analysing the optimum pixel size of the accumulator array corresponding to different parameters at various iterations. In addition, generating rectified ortho-images using matched control linear features will be investigated in future research.

6. REFERENCES

Drewniok, C., and Rohr, K., 1997. Exterior Orientation-An Automatic Approach Based on Fitting Analytic Landmark Models. *ISPRS Journal of Photogrammetry and Remote Sensing*, 52(1997): 132-145.

Fischler, M., and Bolles, R., 1981. Random Sample Consensus: A Paradigm for Model Fitting with Applications to Image Analysis and Automated Cartography. *Communications of the ACM 24*, 6, pp.381-395.

Gülch, E., 1994. Using Feature Extraction to Prepare the Automated Measurement of Control Points in Digital Aerial Triangulation. *International Archives of Photogrammetry and remote Sensing*, Vol. 30, Part 3/1, pp..333-340.

Haala, N., and Vosselman, G., 1992. Recognition of Road and River Patterns by Relational Matching. *International Archives of Photogrammetry and remote Sensing*, Washington, D.C., Vol. 29, Part B, pp.969-975.

Habib, A., 1999. Aerial Triangulation using Point and Linear Features. *International Archives of Photogrammetry and remote Sensing*, München, Germany, Vol. 32, Part 3-2W5, pp.137-141.

Habib, A. and Novak, K., 1994. GPS Controlled Triangulation of Single Flight Lines. *International Archives of Photogrammetry and remote Sensing*, Vol. 30, Part 2, pp.203-209.

Habib, A., Asmamaw, A., and Kelley, D., 2000a. New Approach to Solving Matching Problems in Photogrammetry. *XIXth ISPRS Congress*, Amsterdam, The Netherlands, Vol. 33, Part B2, pp.257-264.

Habib, A., Asmamaw, A., Kelley, D., and May, M., 2000b. *Linear Features in Photogrammetry*. Report No. 450, Department of Civil and Environmental Engineering and Geodetic Science, The Ohio State University, Columbus, Ohio, USA, 80p.

Habib, A., Morgan, M., and Lee, Y., 2001. Integrating Data from Terrestrial Mobile Mapping Systems and Aerial Imagery for Change Detection Purposes. *The 3rd International Symposium on Mobile Mapping Technology*, Cairo, Egypt.

Hough, 1962. *Methods and Means for Recognizing Complex Patterns*, U.S. Patent 3,069,654.

Leavers, V., 1993. Which Hough transformation? *CVGIP Image Understanding*, 41(2): 250-264.

Mikhail, E., 1993. Linear Features for Photogrammetric Restitution and Object Completion. *Integrating Photogrammetric Techniques with Scene Analysis and Machine Vision, SPIE proc.*, Orlando, Florida, USA, No. 1944, pp.16-30.

Mikhail, E., Akey, M., and Mitchell, O., 1984. Detection and Sub-pixel Location of Photogrammetric Targets in Digital Images. *Photogrammetria*, 39(1984): 63-83.

Mulawa, D. and Mikhail, E., 1988. Photogrammetric Treatment of Linear Features. *International Archives of Photogrammetry and remote Sensing*, Vol. 27, Part B3, pp.383-393.

Slama, C., 1980. *Manual of Photogrammetry*, 4th edition, American society of photogrammetry, pp. 574-577.

Zalmanson, G., 2000. *Hierarchical Recovery of Exterior Orientation from Parametric and Natural 3-D Scenes*. Ph. D. Thesis, Department of Civil and environmental Engineering and Geodetic Science, The Ohio State University, Columbus, Ohio, USA, 129p.